

**Acknowledgements**

This work is based on observations obtained with XMM-Newton, an ESA science mission with instruments and contributions directly funded by ESA Member States and the USA (NASA). We thank M. Rees, M. Davies, B. McBreen, R. Willingale and M. Barstow for critical reading of the manuscript, and for discussions.

**Competing interests statement**

The authors declare that they have no competing financial interests..

Correspondence and requests for materials should be addressed to J.N.R.  
(e-mail: jnr@star.le.ac.uk).

## Bunching of fractionally charged quasiparticles tunnelling through high-potential barriers

**E. Comرتی, Y. C. Chung, M. Heiblum, V. Umansky & D. Mahalu**

Braun Center for Submicron Research, Department of Condensed Matter Physics, Weizmann Institute of Science, Rehovot 76100, Israel

Shot noise measurements have been used to measure the charge of quasiparticles in the fractional quantum Hall (FQH) regime<sup>1–3</sup>. To induce shot noise in an otherwise noiseless current of quasiparticles, a barrier is placed in its path to cause weak backscattering. The measured shot noise is proportional to the charge of the quasiparticles; for example, at filling factor  $\nu = 1/3$ , noise corresponding to  $q = e/3$  appears. For increasingly opaque barriers, the measured charge increases monotonically, approaching  $q = e$  asymptotically<sup>4,5</sup>. It was therefore believed that only electrons, or alternatively, three bunched quasiparticles, can tunnel through high-potential barriers encountered by a noiseless current of quasiparticles. Here we investigate the interaction of  $e/3$  quasiparticles with a strong barrier in FQH samples and find that bunching of quasiparticles in the strong backscattering limit depends on the average dilution of the quasiparticle current. For a very dilute current, bunching ceases altogether and the transferred charge approaches  $q = e/3$ . This surprising result demonstrates that quasiparticles can tunnel individually through high-potential barriers originally thought to be opaque for them.

In 1918, Schottky determined the charge of the electron by measuring the average square of the current fluctuations,  $S = \langle i^2 \rangle$ , resulting from the stochastic emission of electrons in a vacuum tube—naming it ‘shot noise’<sup>6</sup>. His expression  $S = 2qI$  is a result of independent random events obeying Poisson distribution. Here,  $S$  is the spectral density of the fluctuations (in units of  $\text{A}^2 \text{Hz}^{-1}$ ),  $q$  is the charge of the particle and  $I$  is the average current. Similar experiments were implemented<sup>1–3</sup> in the FQH regime<sup>7</sup>, verifying the existence of fractionally charged quasiparticles<sup>8</sup>. A partially transmitting constriction, a quantum point contact (QPC), served in these experiments as an adjustable potential barrier in the path of the current, thus partitioning the transmitted charges. This random process is described by a binomial distribution, resulting in  $S = 2qI(1-t)$  at zero temperature, with  $t \in [0, 1]$  being the transmission coefficient of the QPC<sup>4,9,10</sup>. In the weak backscattering regime, the quasiparticles were found to traverse the QPC independently of each other and the measured charge was  $q = e/3$  at filling factor  $\nu = 1/3$  and  $q = e/5$  for  $\nu = 2/5$  (refs 1,2,3). As backscattering gets stronger, the tunnelling of individual quasiparticles becomes correlated, and in the limit of a pinched QPC and

$\nu = 1/3$  three quasiparticles were found to group together to tunnel through the barrier. Obviously, Schottky’s formula is inapplicable for correlated (or bunched) quasiparticles, but it can still be used to characterize the system with the effect of bunching being incorporated into an effective charge  $q(t)$ . Hence, the noise for a pinched QPC becomes electronic-like<sup>4</sup>, that is, with an effective charge of  $q = e$ . Moreover, a nearly universal behaviour was found for the evolution of the effective charge  $q(t)$  (ref. 5), starting at  $q(\text{openQPC}) = e/3$  and monotonically increases toward  $q(\text{pinchedQPC}) = e$ .

Here we explore the bunching properties of a pinched QPC when a sparse beam of  $e/3$  quasiparticles impinges upon it. In other words, when there are not enough quasiparticles in close proximity to bunch into an ‘electron’, we may ask the following questions: (1) will

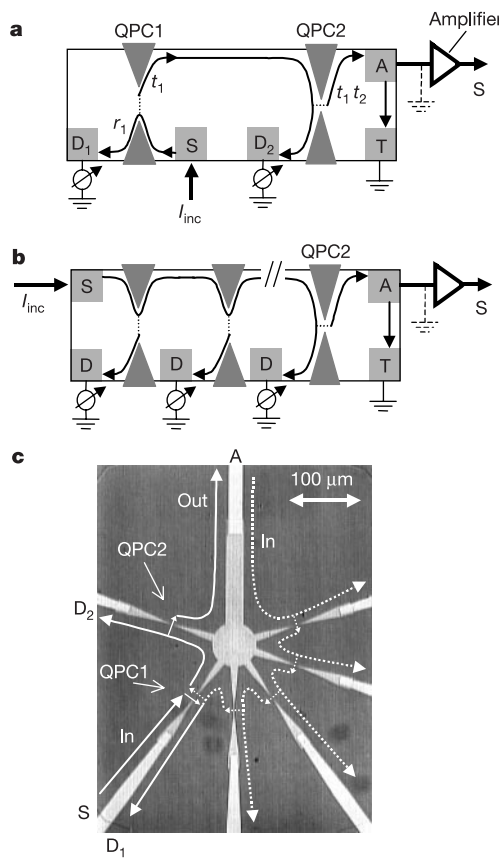


**Figure 1** Schematic and actual representations of the quasiparticle injector followed by a quasiparticle filter, both made of quantum point contacts. QPC1 and QPC2, respectively. **a**, An injector made of a relatively open QPC1 partitions an incident noiseless (d.c.) current, injected from source terminal S. The scattered part ( $t_1$ ), composed of a dilute beam of quasiparticles, impinges on a pinched QPC2. The resulting noise is measured by a cooled, low-noise, amplifier at terminal A (see ref. 1). The intermediate drain  $D_2$  prohibits multiple reflections, and the grounded terminal T is used to fix the output impedance of the sample and make it independent of QPC settings. **b**, An alternative scheme, suitable for producing a moderately dilute current, invokes a cascade of weakly backscattering QPCs transmitting a dilute quasiparticle beam (see ref. 11). **c**, A photograph of the actual device in the vicinity of the QPCs, formed by metallic gates (light grey regions) deposited on the surface of the GaAs-AlGaAs heterostructure, embedding a two-dimensional electron gas some  $0.1 \mu\text{m}$  below the surface. Electron mobility is  $2 \times 10^6 \text{ cm}^2 \text{V}^{-1} \text{s}^{-1}$  and areal carrier density is  $1.1 \times 10^{11} \text{ cm}^{-2}$ , both measured at  $4.2 \text{ K}$  in the dark. The solid arrows correspond to the direction of current in configuration **a**, and the other QPCs on the right (with current flow denoted by dotted arrows) are used when configuration **b** is employed. Ohmic contacts (serving as S, D, T, A) are outside the frame of the picture.

the barrier become opaque? (2) Will quasiparticles be ‘borrowed’ from lower-energy states to fill in for the missing ones in the beam? Or, (3) perhaps the bunching condition will be relaxed and individual quasiparticles will transverse the barrier? Theory does not yet provide answers to these questions.

Samples were fabricated in a high-mobility two-dimensional electron gas embedded in a GaAs–AlGaAs heterostructure. Measurements were done in a strong magnetic field of  $B \approx 13$  T and a fractional filling factor of  $\nu = 1/3$  in the FQH regime. Vanishing of the longitudinal resistivity  $\rho_{xx}$  ensures that the (net) current is flowing chirally along the edges of the sample in edge states. This allows measurements in multi-terminal geometries, shown in Fig. 1. Two techniques are used to partition the quasiparticle beam, hence making it sparse or dilute, before it impinges on the pinched QPC2. A straightforward scheme, shown in Fig. 1a, uses a noiseless current  $I_{\text{inc}}$  that impinges on a relatively open QPC1 and partially scatters toward QPC2 (although in this case the small reflection coefficient of QPC1 is responsible for the dilution of the current, for uniformity we stick to the notation of transmission coefficient  $t_1 \rightarrow 0$ ). Most of the current continues toward drain  $D_1$ ; the scattered part toward QPC2 is a very dilute beam of quasiparticles with charge  $q_1 = e/3$  (refs 1, 2, 5) and dilution determined by  $t_1$ . Much of that dilute current is reflected back by QPC2 toward drain  $D_2$  and a small part  $t_2$  is transmitted. A fraction  $t_1 t_2$  of the incident current reaches the amplifier. This method cannot be applied, however, to achieve a moderately sparse beam of quasiparticles since a partly pinched QPC1 would lead to bunching of quasiparticles and to an effective charge of  $q_1 > e/3$  (ref. 5). Hence, we also use a geometry shown in Fig. 1b. Here, the incident current is being partitioned by transmission through a cascade of weakly backscattering QPCs (for each  $t_1 \rightarrow 1$ ), feeding QPC2 with a current

of quasiparticles with arbitrary dilution  $t_1 = \prod_i t_i$ . The fact that the partitioned charge by this method is  $e/3$  is not obvious and a detailed study<sup>11</sup> was needed to prove that a beam of quasiparticles is indeed produced. We also tested, through detailed noise measurements<sup>11</sup>, whether dilute quasiparticles suffer intra-edge scattering and subsequent equilibration during transport along the device edges. Equilibration establishes a new chemical potential and increases the occupation of each state below the chemical potential, hence modifying the dilution of the beam. As shown in ref. 11, such equilibration does not take place in our devices.

Using one of the two methods depicted in Fig. 1, we create a noisy beam of quasiparticles with charge  $e/3$ , which is being further partitioned by QPC2. The noise at amplifier A is measured with a spectrum analyser after amplification by a cooled amplifier. The amplifier, being placed near the sample, has a very low current noise at its input,  $\langle i_{\text{amp}}^2 \rangle = 1.5 \times 10^{-28} \text{ A}^2 \text{ Hz}^{-1}$ , when operating with a bandwidth of 30 kHz and centre frequency  $f_0 \approx 1.5$  MHz. The value of  $f_0$ , chosen well above the cut-off of the ubiquitous  $1/f$  noise, is determined by a resonance of  $LC$  circuit, with  $C$  the capacitance of the coaxial cable connecting the sample and the amplifier and  $L$  the inductance of an added superconducting coil<sup>1</sup>. Reflected currents flow into the grounded terminals D and T, leading to a constant input (at S) and output (at A) conductance  $G = e^2/3h$  that is independent of the transmission of the QPCs. This makes both the sample’s equilibrium noise ( $4k_B T G = 5 \times 10^{-29} \text{ A}^2 \text{ Hz}^{-1}$ ) and the sample-dependent amplifier’s noise ( $\langle i_{\text{amp}}^2 \rangle/G^2$ ) independent of the transmission of the QPCs, allowing subtraction of both from the measured noise (for comparison, the magnitude of the shot noise at A is typically in the  $10^{-30} \text{ A}^2 \text{ Hz}^{-1}$  range).  $k_B$  is Boltzmann’s constant.

The configuration in Fig. 1a can be analysed by means of superposition<sup>12</sup>. Consider first the ‘injector’ QPC1, characterized by transmission  $t_1 \rightarrow 0$  toward QPC2 and partitioned charge  $e/3$ . Because QPC1 is a stochastic element, it generates (at zero tem-

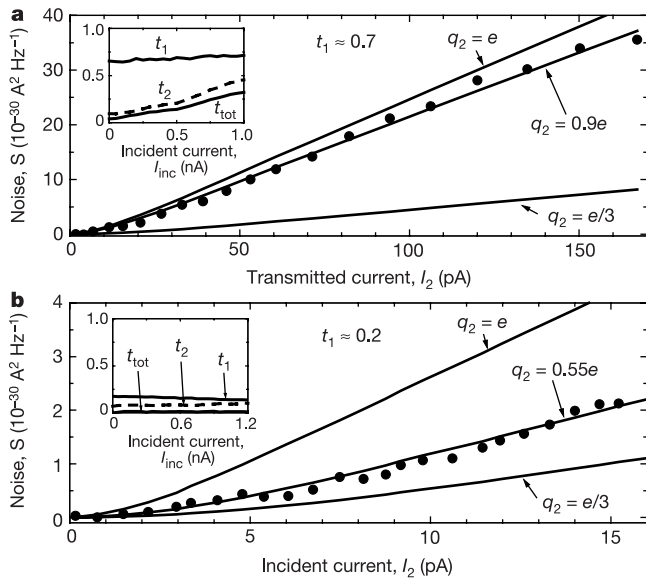


**Figure 2** Noise and transmission measurements of the pinched QPC2 (with transmission  $t_2 \approx 0.1$  at zero bias) for two different values of dilution of the impinging current:  $t_1 = 0.7$  (a) and  $0.2$  (b). In the main graphs the measured noise is plotted against the transmitted current, together with the theoretical prediction of the independent particles model at a finite temperature. The intermediate curve in each graph represents the best fit to an arbitrary charge  $q_2$ . Various transmission coefficients, measured simultaneously with the noise, are shown in the insets against the incident (noiseless) current. Each inset shows the dilution level  $t_1$  generated by the QPC1 injector, the transmission  $t_2$  of the pinched QPC2 in response to the dilute impinging current, and the total transmission  $t_{\text{tot}}$ . We note that the sensitivity of  $t_2$  to the current depends on the dilution level of the impinging current.

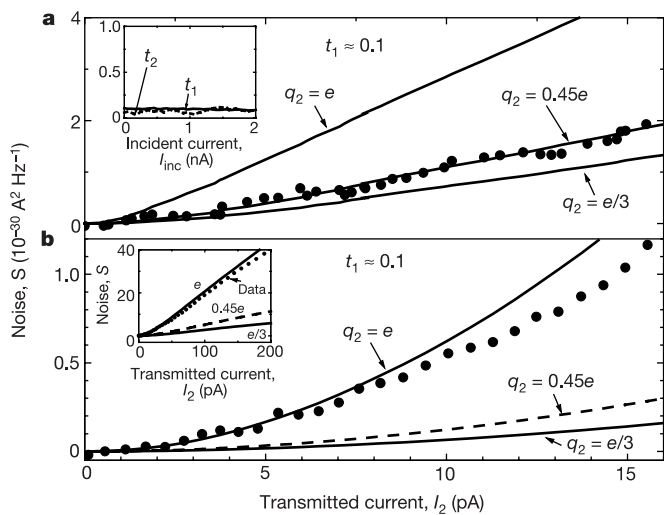


**Figure 3** Comparison of the charge characterizing the pinched QPC2 for two extreme cases of the impinging current: not diluted (noiseless) and highly dilute, keeping the same transmitted current. a, The noise produced by the pinched QPC2 when fed by a highly dilute impinging current,  $t_1 \approx 0.1$ , corresponds to a quasiparticle charge  $q_2 = 0.45e$ . The inset shows the current-dependent transmission  $t_1$  (level of dilution) and the transmission  $t_2$  (which is fairly current-independent for such a dilute beam). b, The noise produced by the pinched QPC2 when fed by a noiseless current corresponds to an almost electronic charge. The inset verifies the charge  $q_2 = e$  by measuring the noise over a considerably wider range of transmitted current. Clearly, the charge characterizing QPC2 depends not only on the potential barrier height but also on the average occupation of the states (dilution) of the impinging current.

perature) noise  $2(e/3)I_{\text{inc}}t_1(1 - t_1)$ , with  $I_{\text{inc}}t_1$  the transmitted current, impinging on QPC2. This noise is attenuated with a factor  $t_2^2$  by QPC2, resulting in a contribution of QPC1 to the total noise:

$$S_1 = 2(e/3)I_{\text{inc}}t_1(1 - t_1)t_2^2 \quad (1)$$

Consider now QPC2, characterized by transmission  $t_2$  and charge  $q_2$  when impinged by a noiseless current  $I_{\text{imp}}$  of  $e/3$  quasiparticles. It produces noise  $2q_2I_{\text{imp}}t_2(1 - \tilde{t}_2)$ , where  $I_{\text{imp}}t_2 = I_2$  is the transmitted current and  $\tilde{t}_2 = t_2[(e/3)/q_2]$  denotes the effective transmission for charge  $q_2$  quasiparticles. This transmission  $\tilde{t}_2$  is determined self-consistently with the charge  $q_2$  in order to maintain the measured conductance of QPC2 (ref. 5). We stress that even though the current  $I_{\text{imp}} = I_{\text{inc}}t_1$  is noisy we still use the above expression to calculate the noise generated by QPC2, because the noise in  $I_{\text{imp}}$  was already taken into account in equation (1). The added contribution of QPC2 is therefore:

$$S_2 = 2q_2I_{\text{inc}}t_1t_2(1 - \tilde{t}_2) \quad (2)$$

The total noise in A is then  $S_1 + S_2$ . The correctness of this analysis can be validated in the limit of a constant charge (say,  $e/3$ ):  $S_1 + S_2 = 2(e/3)I_{\text{inc}}t_1t_2(1 - t_1t_2)$ , with  $t_{\text{tot}} = t_1t_2$  being the total transmission from S to A—the standard expression for a binomially distributed process. In the experiment we use the expression for  $S_1 + S_2$  in order to determine the charge  $q_2$  partitioned by QPC2. In the limit where both  $t_1$  and  $t_2$  are small,  $S_1$  and  $S_2$  are of the order of  $O(t_1t_2^2)$  and  $O(t_1t_2)$ , respectively, with the  $S_1$  much smaller than  $S_2$ . Hence, the measured noise is dominated by the contribution of the pinched QPC2:

$$S \equiv 2q_2I_{\text{inc}}t_1t_2 = 2q_2I_2 \quad (3)$$

We verify first that the noise produced by a pinched QPC, when fed with a quiet current, corresponds as expected to  $q \approx e$ . We find results similar to these in ref. 5 with an example given in Fig. 3b. For  $t_1 = 1$ , hence feeding QPC2 with a noiseless current, and  $t_2 \approx 0.1$ , we measure indeed charge  $e$ . We then partition the incident current by setting  $t_1 < 1$ , and hence impinging a noisy current of quasiparticles on QPC2 with  $t_2 \approx 0.1$ . Two examples are shown in Fig. 2, one for average state occupation  $t_1 \approx 0.7$  (Fig. 2a) and one for  $t_1 \approx 0.2$  (Fig. 2b). When calculating the expected noise<sup>5</sup> we take into

account the finite temperature of the electrons ( $T \approx 65$  mK) and the energy (or current) dependence of the total transmission  $t_{\text{tot}} = t_1t_2$  (current-dependent transmissions are shown in the insets of Fig. 2). The average current is being varied over a large enough range, with the voltage  $V$  satisfying  $q_2V \gg k_B T$ , to allow the noise to reach the linear regime. Nice agreement is found between the data and the independent particle model for  $q_2 = 0.9e$  and  $t_1 \approx 0.7$  (lightly diluted current) and for  $q_2 = 0.55e$  and  $t_1 \approx 0.2$  (highly diluted current).

A more striking example of the effect of beam dilution is demonstrated in Fig. 3, where the range of current  $I_2$  is kept constant for different values of dilution. Obviously, a higher source voltage is required to obtain the same current  $I_2$  when the current is more dilute. In comparison with the measured electron charge for a noiseless impinging current (Fig. 3b), a highly dilute current ( $t_1 \approx 0.1$ ) impinging on the pinched QPC2 is found to produce a small charge  $q_2 = 0.45e$  (Fig. 3a)—slightly above the charge of the quasiparticles.

Figure 4 summarizes the dependence of  $q_2$  on the dilution  $t_1$  of the impinging current on QPC2. Two examples,  $t_2 = 0.1$  and  $t_2 = 0.25$ , are chosen, with corresponding charge  $e$  and  $0.75e$ , respectively, for a noiseless impinging current. The more dilute the impinging current is ( $t_1 \rightarrow 0$ ), the smaller is the effective charge  $q_2$ —approaching  $\sim e/3$  asymptotically. We conclude that bunching of quasiparticles is not an essential mechanism for the transfer of quasiparticles through high-potential barriers. Bunching takes place only when the incoming states are highly occupied.

We also wondered how the transmission of QPC2 is affected by the dilution of the impinging quasiparticles. Present theory assumes only a noiseless current approaching a constriction within the framework of the Luttinger model. Here we also find counter-intuitive results. In the linear regime, where the source voltage is small enough to keep the transmission almost energy-independent (Fig. 5a), the transmission  $t_2$  is independent of dilution (although the source voltage for the dilute current is some ten times larger). This can be compared with the case where the same source-voltage range is kept (Fig. 5b). Here, the transmission  $t_2$  of the noiseless current strongly depends on voltage (approaching unity at  $V > 50$   $\mu$ V). Equilibration of quasiparticles had been ruled out<sup>11</sup>,

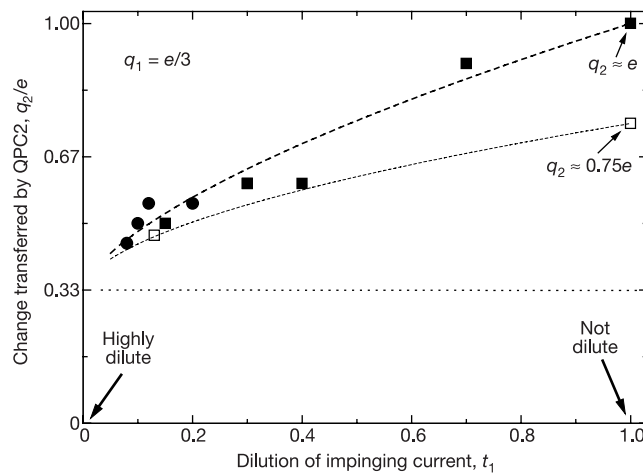


**Figure 4** Evolution of the effective charge  $q_2$  that characterizes the pinched QPC2 in response to different values of dilution  $t_1$  of the impinging current (extracted from curves similar to that in Fig. 3a). Results of three different measurements are shown—two complementary sets of data for  $t_2 = 0.1$  (filled squares and circles), with dilution produced by backscattering of a single QPC1 (circles, Fig. 1a) and by transmission through five, relatively open, QPCs (squares, Fig. 1b), and one set with  $t_2 = 0.25$ . In the case of  $t_2 = 0.25$  only the extreme points are shown in order to simplify the graph (open

squares). The dashed lines are only a guide to the eye. Evidently, as the current impinging on the pinched QPC2 becomes more dilute, the charge drops from its original value toward  $\sim e/3$  in the limit of very high dilution. We conclude that individual, very sparse, quasiparticles tunnel through a pinched QPC that was originally thought to be opaque for them. Filled circles and squares,  $t_2 = 0.1$  and  $q_2(\text{not dilute}) = e$ . Open squares,  $t_2 = 0.25$  and  $q_2(\text{not dilute}) = 0.75e$ .

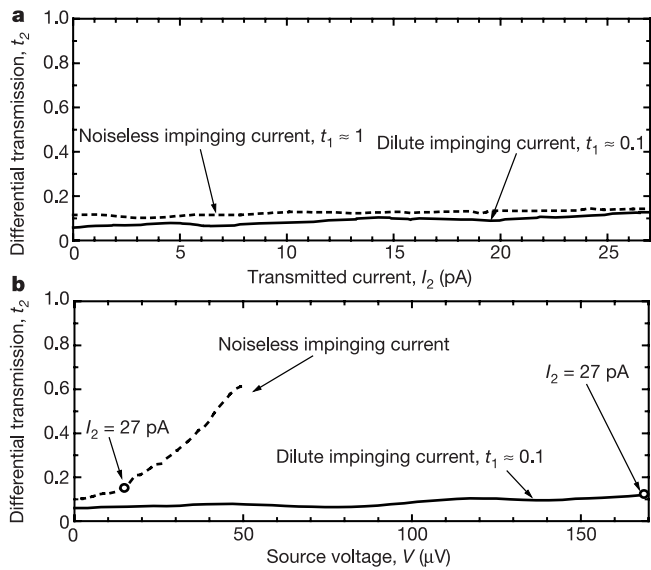


**Figure 5** Dependence of the transmission  $t_2$  of the pinched QPC2 on the dilution  $t_1$  of the impinging current. **a**, Measurements in the linear regime. The transmission  $t_2$  of a highly dilute impinging current ( $t_1 \approx 0.1$ , solid curve) and that of a noiseless current ( $t_1 = 1$ , dashed curve), with the same transmitted current range kept in both cases. The applied source voltage, on the other hand, reaches a maximal value of  $\sim 170$   $\mu$ V for the noisy impinging current but only  $\sim 16$   $\mu$ V in the noiseless case. Nevertheless, the transmissions in both cases are similar. **b**, Measurements in the nonlinear regime. Similar measurements to **a** but the same applied source voltage range is kept in both cases (the noiseless current is some ten times larger for the same voltage). The transmission is found to be strongly current-dependent when the impinging current is noiseless.

so we conclude that the nonlinearity of the pinched QPC depends strongly on the quasiparticle current and less on the quasiparticle energy. This rules out that the potential profile of the barrier in the QPC is responsible for the nonlinearity of the current. Moreover, the insensitivity of the transmission  $t_2$  in the linear regime to the dilution of the impinging quasiparticle beam suggests equal probabilities of tunnelling for a single quasiparticle and for bunched quasiparticles. In other words, noise and transmission measurements show that quasiparticles can transfer, with the same ease, either one by one or bunched in groups. Their bunching depends on the transparency of the barrier and on the preparation of the quasiparticle beam. It is now for theory to explain such a bizarre effect.

Received 6 November 2001; accepted 20 February 2002.

1. de Picciotto, R. *et al.* Direct observation of a fractional charge. *Nature* **389**, 162–164 (1997).
2. Saminadayar, L., Glattli, D. C., Jin, Y., Etienne, B. Observation of the  $e/3$  fractionally charged Laughlin quasiparticle. *Phys. Rev. Lett.* **79**, 2526–2529 (1997).
3. Reznikov, M., de-Picciotto, R., Griffiths, T. G., Heiblum, M. & Umansky, V. Observation of quasiparticles with one-fifth of an electron's charge. *Nature* **399**, 238–241 (1999).
4. Kane, C. L. & Fisher, M. P. A. Nonequilibrium noise and fractional charge in the quantum Hall effect. *Phys. Rev. Lett.* **72**, 724–727 (1994).
5. Griffiths, T. G., Compti, E., Heiblum, M., Stern, A. & Umansky, V. Evolution of quasiparticle charge in the fractional quantum Hall regime. *Phys. Rev. Lett.* **85**, 3918–3921 (2000).
6. Schottky, W. Über spontane Stromschwankungen in verschiedenen Elektrizitätsleitern. *Ann. Phys. (Leipzig)* **57**, 541–567 (1918).
7. Prange, R. E. & Girvin, S. M. (eds) *The Quantum Hall Effect* (Springer, New York, 1987).
8. Laughlin, R. B. Anomalous quantum Hall effect: an incompressible quantum fluid with fractional charge excitations. *Phys. Rev. Lett.* **50**, 1395–1398 (1982).
9. Khlas, V. K. Current and voltage fluctuations in microjunctions of normal and superconducting metals. *Sov. Phys. JETP* **66**, 1243–1249 (1987).
10. Lesovik, G. B. Excess quantum noise in 2D ballistic point contacts. *JETP Lett.* **49**, 592–594 (1989).
11. Compti, E., Chung, Y. C., Heiblum, M. & Umansky, V. Multiple scattering of fractionally-charged quasiparticles. Preprint cond-mat/0112367 at <http://xxx.lanl.gov> (2001).
12. Oliver, W. D., Kim, J., Liu, R. C. & Yamamoto, Y. Hanbury Brown and Twiss-type experiment with electrons. *Science* **284**, 299–301 (1999).

## Acknowledgements

The work was partly supported by the Israeli Academy of Science and by the German-Israel Foundation (GIF). We thank A. Yacoby, A. Stern and Y. Levinson for discussions.

## Competing interests statement

The authors declare that they have no competing financial interests.

Correspondence and requests for materials should be addressed to M.H. (e-mail: heiblum@wisemail.weizmann.ac.il).

## Atomic-scale images of charge ordering in a mixed-valence manganite

**Ch. Renner\*, G. Aepli\*, B.-G. Kim†, Yeong-Ah Soh\* & S.-W. Cheong†**

\* NEC Research Institute, 4 Independence Way, Princeton, New Jersey 08540, USA  
† Rutgers University, Department of Physics and Astronomy, Piscataway, New Jersey 08854, USA

Transition-metal perovskite oxides exhibit a wide range of extraordinary but imperfectly understood phenomena. The best known examples are high-temperature superconductivity in copper oxides<sup>1</sup>, and colossal magnetoresistance in manganese oxides ('manganites')<sup>2,3</sup>. All of these materials undergo a range of order-disorder transitions associated with changes in charge, spin, orbital and lattice degrees of freedom. Measurements of such order are usually made by diffraction techniques, which detect the ionic cores and the spins of the conduction electrons. Unfortunately, because such techniques are only weakly sensitive to valence electrons and yield superpositions of signals from distinct submicrometre-scale phases, they cannot directly image phase coexistence and charge ordering, two key features of the manganites. Here we present scanning tunnelling microscope measurements of the manganite  $\text{Bi}_{1-x}\text{Ca}_x\text{MnO}_3$ . We show that charge ordering and phase separation can be resolved in real space with atomic-scale resolution. By taking together images and current-voltage spectroscopy data we find that charge order correlates with both structural order and the local conductive state (either metallic or insulating). These experiments provide an atomic-scale basis for descriptions<sup>4</sup> of manganites as mixtures of electronically and structurally distinct phases.

The material chosen for our experiments is  $\text{Bi}_{1-x}\text{Ca}_x\text{MnO}_3$  (BCMO). For trivalent Bi and divalent Ca, the Mn ions are in a mixed valence state,  $\text{Mn}^{3+,\text{4+}}$ . At high temperature,  $\text{Mn}^{3+}$  and  $\text{Mn}^{4+}$  randomly occupy the manganese sites. Upon reducing the temperature, these cations are believed to order, yielding an increased lattice periodicity visible to X-ray and neutron diffraction<sup>5</sup>. For our samples of nominal  $x = 0.76$ , grown from a BiO flux, this occurs at  $T_{\text{CO}} = 250$  K, as established using SQUID (superconducting quantum interference device) magnetometry. We performed the scanning tunnelling microscope (STM) experiments in ultrahigh vacuum at a base pressure of  $5 \times 10^{-10}$  torr. Previously published STM investigations of manganites primarily focused on spectroscopy of the density of states averaged over many atoms<sup>6,7</sup>, and demonstrated phase separation into metallic and insulating regions on submicrometre<sup>8</sup>, but not atomic, length scales. In contrast, STM with atomic resolution has already been achieved for copper oxides, and revealed inhomogeneities in the superconducting order on atomic length scales<sup>9,10</sup>.

Single crystals of BCMO do not cleave naturally, and preparing